Draft version September 8, 2014
Preprint typeset using LaTeX style emulateapj v. 5/2/11

arXiv:1409.1791v1 [astro-ph.GA] 5 Sep 2014

ON ASYMMETRIC DISTRIBUTIONS OF SATELLITE GALAXIES

A. Bowden[1], N.W. Evans[1], V. Belokurov[1]
Institute of Astronomy, University of Cambridge, Madingley Road, Cambridge CB3 0HA, UK
Draft version September 8, 2014

ABSTRACT

We demonstrate that the asymmetric distribution of M31 satellites cannot be produced by tides from the Milky Way as such effects are too weak. However, loosely bound associations and groups of satellites can fall into larger haloes and give rise to asymmetries. We compute the survival times for such associations. We prove that the survival time is always shortest in Keplerian potentials, and can be ~ 3 times longer in logarithmic potentials. We provide an analytical formula for the dispersal time in terms of the size and velocity dispersion of the infalling structure. We show that, if an association of ~ 10 dwarfs fell into the M31 halo, its present aspect would be that of an asymmetric disk of satellites. We also discuss the case of cold substructure in the Andromeda II and Ursa Minor dwarfs.
Subject headings: galaxies: kinematics and dynamics — Local Group — galaxies: dwarf – galaxies: individual: M31

1. INTRODUCTION

Asymmetric distributions of satellite galaxies are seemingly common. McConnachie & Irwin (2006) found that all bar one of the known 16 satellites of M31 lie on the hemisphere of the M31 sky facing the Milky Way Galaxy. The more recent investigation of Conn et al. (2013) using a larger sample has soothed worries that this was an artefact of small sample size or observational bias. Ibata et al. (2013) analyzed the radial velocities of the satellites and argued that 13 of the satellites possess a coherent rotational motion, with 12 of the 13 lying on the side of M31 nearest to the Milky Way Galaxy.

For our Galaxy, there are also tantalizing hints of a similar asymmetric distributions, though our 'fishbowl' viewpoint makes such claims hard to evaluate. Plots of the locations of the known Milky Way satellites in the sky seem to suggest that the northern Galactic hemisphere is over-endowed compared to the southern. Most of the northern Galactic hemisphere lies on the far side of the Milky Way as judged from an M31 perspective. In other words, the Milky Way satellites are also asymmetrically distributed with a preponderance on the far side from M31.

What causes such asymmetries in satellite distributions to be set up and how do they maintain themselves? At first sight, tidal forces suggest themselves as a possibility. Suppose the Milky Way and M31 have mass M and separation D in the x-direction, then the tidal potential in the frame of the host is

$$\Phi_{\rm tidal} = -\frac{GM}{\sqrt{(D-x)^2+y^2+z^2}}. \qquad (1)$$

Using a Taylor expansion in the limit $x, y, z \ll D$ for a distant perturber, the tidal force is

$$F_x = \frac{GM}{D}\left(\frac{1}{D} + \frac{2x}{D^2} + \frac{3x^2}{D^3} - \frac{3y^2}{2D^3} - \frac{3z^2}{2D^3}\right). \qquad (2)$$

The first term here is GM/D^2. As this calculation is done in the frame of the host galaxy, this cancels with the acceleration due to the non-inertial frame. We then have several terms which are linear in x and these cannot lead to an asymmetry in the satellite population. The lowest order term that can generate any asymmetry is the $3GMx^2/D^4$ term. The magnitude of this effect for a Milky Way-M31 pair is roughly ~ 1 kpc, as can be verified by simulations in the center of mass frame of the Milky Way and M31. This is clearly insufficient to explain the asymmetry in the population of M31 satellites.

This leads us to consider the possibility that such asymmetries arise from the initial conditions of infall of satellites. Significant fractions of satellites may be accreted from a similar direction in groups, or in loosely bound associations or clumps and this can lead to asymmetries in the satellite distributions (e.g., Li & Helmi 2008; D'Onghia & Lake 2008). Motivated by the example of M31, Shaya & Tully (2013), Goerdt & Burkert (2014) and Sadoun, Mohayaee & Colin (2014) provide scenarios in which groups of satellite galaxies may be accreted in preferred directions. Libeskind et al. (2011) demonstrate that in simulations of the Local Group, satellite infall is not spherical in nature and that preferred directions are observed. Bahl & Baumgardt (2014) show that planar features are not uncommon in cosmological simulations, however the features they describe are transient in nature. The extent to which such associations and phase space structures can persist over a Hubble time without dispersal through phase-mixing is not immediately an obvious.

2. THE DISPERSAL THEOREM

An observable asymmetry may indicate that an initially clumpy population has not had sufficient time to fully phase mix. This suggests that we examine the dispersal of such clumps. The most natural coordinate system in which to do so is action-angles. Here, actions are conserved while angles evolve linearly with time (see e.g., Goldstein 1980)

$$\theta = \theta_0 + \omega t. \qquad (3)$$

Let us consider the dispersal of a clump in action-angle space. For our application, the clump is composed of a loose association of satellite galaxies, though the theorem

nwe@ast.cam.ac.uk

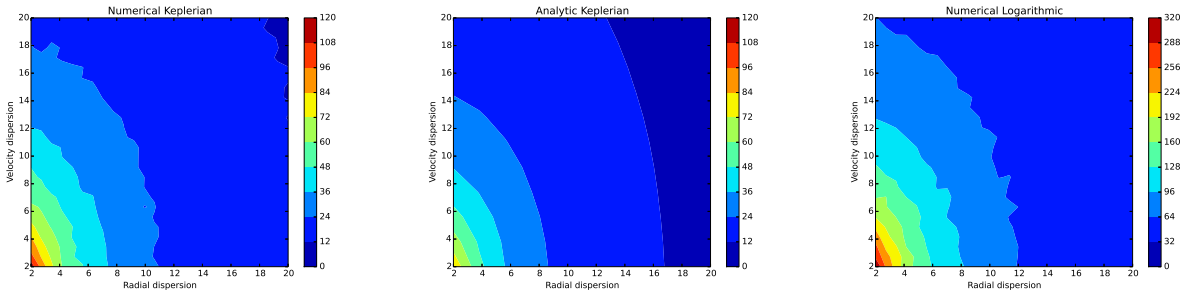

FIG. 1.— Contour plots showing the time taken for the rms $\Delta\phi$ to reach 2π as a function of dispersion in position σ_r and velocity σ_v of the Gaussian clump of eq. (14) for (left, middle panels) Keplerian and (right panel) logarithmic potentials. The left and right panels have been computed by direct simulation, whilst the middle panel uses the analytic formula of eq. (14). All the panels refer to the case of a $10^{10}M_\odot$ association, which is placed on an orbit with $\mu_r = 200$ kpc and $\mu_v = 150$ kms^{-1}. This is tailored for the case of dispersal of an assemblage of dwarf galaxies in the outer parts of the halo of a galaxy like M31.

we prove holds more generally. As the clump disperses, the spread in actions (which are adiabatic invariants) is conserved, whilst the spread in angles is

$$\Delta\theta = \delta\theta_0 + \delta\omega t. \tag{4}$$

So, the dispersal of the clump in time therefore only depends on $\delta\omega$, the difference in frequencies as actions are changed by a small amount, that is, the Hessian matrix multiplied by the difference in actions. This is similar to the related problem in stream dynamics (c.f., Sanders & Binney 2013).

We can compute the Hessian for scale-free power-law potentials (Evans 1994), which take the form:

$$\Phi(r) = Ar^\alpha, \qquad A = \frac{v_0^2}{\alpha r_0^\alpha}. \tag{5}$$

Here, v_0 is the circular velocity at radius r_0. When $\alpha = 0$, this becomes the isothermal sphere, whilst when $\alpha = -1$ this is of course the Kelperian case. The outer parts of galaxy haloes lie between these two limiting cases.

In a spherical potential, there are two actions, namely the radial action J_r and the azimuthal action J_ϕ which may be taken as the angular momentum L (see e.g., Goldstein 1980). The Hamiltonian as a function of the actions takes the form (Williams, Evans & Bowden 2014)

$$H(L, J_r) = C(J_\phi + DJ_r)^\beta, \tag{6}$$

Here, $\beta = 2\alpha/(\alpha+2)$ and the constants C and D are given in Williams et al (2014). Differentiation gives the angular frequency as

$$\omega_\phi = (A\alpha)^{2/(\alpha+2)}(J_\phi + DJ_r)^{(\alpha-2)/(\alpha+2)}. \tag{7}$$

One more differentiation gives the components of the Hessian

$$\frac{\partial^2 H}{\partial J_\phi \partial J_i} = (A\alpha)^{2/(\alpha+2)}\frac{\alpha-2}{\alpha+2}a_i(J_\phi + DJ_r)^{-4/(\alpha+2)}, \tag{8}$$

where a_i is D for J_r and 1 for J_ϕ. This is a decreasing function of α if the power-law models are normalised to the same enclosed mass. *So, for a fixed enclosed mass, the closer the potential is to Keplerian, the larger the magnitude of the Hessian and the faster the dispersal.* This is the dispersal theorem.

We may be interested in the number of orbits $n_{\rm orb}$ it takes for a clump to spread out. This means we divide out the frequency ω_ϕ by the Hessian matrix,

$$n_{\rm orb} \propto \omega_\phi(\frac{\partial^2 H}{\partial J_\phi \partial J_i})^{-1} = \frac{\alpha+2}{\alpha-2}\frac{(J_\phi + DJ_r)}{a_i}. \tag{9}$$

As D increases as a function of α, it is straightforward to establish that the complete expression is an increasing function of α. In other words, the Keplerian case is again the most efficient at mixing.

An assumption in these calculations is that the spread in angles dominates the evolution of the clump, whilst the spread in actions is small. This assumption is likely to hold good for small clumps. Therefore, it is important to test the results against simulations, which we proceed to do in the next section.

3. THE DISPERSAL OF GROUPS OF SATELLITES

3.1. *Keplerian Case*

To describe the degree of phase mixing as a clump disperses, we use the mean angular separation between galaxies in the association. This can be computed both analytically and numerically. We consider phase mixing to be complete when this value reaches 2π.

To start with, we assume the simplest case of a Keplerian galactic host potential. In this potential, orbits have periods given by

$$P_{\rm orb} = \frac{\pi GM}{\sqrt{2}}\epsilon^{-3/2}, \tag{10}$$

where ϵ is the energy and M is the mass of the host galaxy. Provided the orbit is not highly eccentric, then the angular phase is

$$\phi \approx \frac{2\pi t}{P_{\rm orb}} = \frac{2\sqrt{2}}{GM}\epsilon^{3/2}t. \tag{11}$$

The magnitude of the difference in ϕ between two such satellites is

$$(\Delta\phi)^2 = A(\epsilon_1^{3/2} - \epsilon_2^{3/2})^2 = A(\epsilon_1^3 + \epsilon_2^3 - 2\epsilon_1^{3/2}\epsilon_2^{3/2}), \tag{12}$$

where $A = 8t^2/(G^2M^2)$. To find the mean, we integrate over phase space co-ordinates after multiplying by a probability distribution. We model the group of satellites as a (truncated) Gaussian with dispersions in position and velocity σ_r and σ_v around means μ_r and μ_v

$$P = \frac{1}{(2\pi\sigma_r\sigma_v)^2}\exp -\left(\frac{(r_1-\mu_r)^2}{2\sigma_r^2}\right. \tag{13}$$

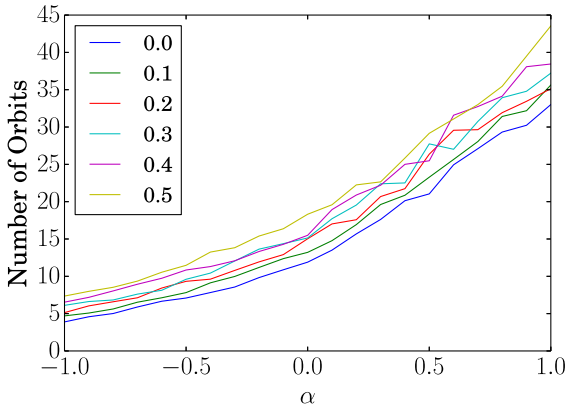

FIG. 2.— Plot showing the number of orbits required for a Gaussian clump to phase mix as a function of power-law index for scale-free spherical potentials. The mean position and rotational velocity of the clump is the same as in Fig. 1. Different lines correspond to different orbital eccentricities for the clump. We observe that the efficiency of phase mixing is an increasing function of power-law index α, with the Keplerian case as the fastest dispersing. This vindicates the dispersal theorem.

$$+\frac{(r_2-\mu_r)^2}{2\sigma_r^2}+\frac{(v_1-\mu_v)^2}{2\sigma_v^2}+\frac{(v_2-\mu_v)^2}{2\sigma_v^2}\Bigg).$$

We thus evaluate numerically

$$\overline{(\Delta\phi)^2}=A\int P(\epsilon_1^3+\epsilon_2^3-2\epsilon_1^{3/2}\epsilon_2^{3/2})dr_1dr_2dv_1dv_2. \quad (14)$$

truncating our probability distribution at 4σ.

3.2. *Logarithmic Case*

For arbitrary spherical potentials, such as the flat rotation curve or logarithmic case, we must evaluate

$$\overline{(\Delta\phi)^2}=C\int P\left(\frac{1}{T_{\phi_1}^2}+\frac{1}{T_{\phi_2}^2}-\frac{1}{T_{\phi_1}T_{\phi_2}}\right)dr_1dr_2dv_1dv_2. \quad (15)$$

Here, T_ϕ is the azimuthal period, given by $T_\phi = 2\pi T_r/|\Delta\phi|$, with

$$T_r=2\int_{r_1}^{r_2}\frac{dr}{\sqrt{2[E-\Phi(r)]-L^2/r^2}}, \quad (16)$$

and

$$\Delta\phi=2L\int_{r_1}^{r_2}\frac{dr}{r^2\sqrt{2[E-\Phi(r)]-L^2/r^2}}. \quad (17)$$

The validity of these approximations can be tested via direct comparison to numerical simulations. The simulations involve drawing test particles from a 6-D Gaussian centered on the mean position and velocity. These particles are integrated forwards in time in the host galactic potential, assuming no self-gravity, and their mean angular separation evaluated.

Fig. 1 shows the time taken in the Keplerian and logarithmic cases for the mean $\Delta\phi$ to reach 2π, for a range of values of σ_r and σ_v. In each case, the clump is centered on an orbit with $\mu_r = 200$ kpc and $\mu_v = 150$ kms^{-1}, as might be appropriate for the outer parts of a large galaxy like M31. The enclosed mass of the host galaxy is $M = 2.2\times10^{12}M_\odot$, comparable to estimates of the mass of M31 (see e.g., Evans & Wilkinson 2000; Diaz et al. 2014). The analytic approximation reproduces well the shape of the contours, however it slightly underestimates the time taken for a clump to disperse. The likely sources of the discrepancy are the approximations we have made, particularly the assumption that the angular velocity of the particles is constant in time, allowing us to perform our integrals in terms of the angular period. Further, we modeled our probability distribution as Gaussian in the magnitude r and v. This requires the implicit assumption that our perturbations about the mean clump velocity are in the direction of motion, and perturbations about the position are radial. In actuality, we should perform an integral over the 6-D phase space. However, perturbations to the relevant quantities or r and v from a six-dimensional Gaussian are dominated by the contributions from the radial position terms and the direction of motion velocity terms.

Fig. 2 shows, for the same clump mean velocities, the number of orbits required for the mean $\Delta\phi$ to reach 2π for a variety of power-law potentials as given in eq (5). This demonstrates that the number of orbital periods needed for dispersal is an increasing function of α, as suggested by our calculation in Section 2. Note that the simulations have really pushed beyond the frozen action approximation used there. Comparing the Keplerian and Logarithmic potentials – which are the likely bounding cases for the outer parts of galaxy haloes – an identical clump takes more orbital periods to disperse in the logarithmic halo by a factor of ~ 3.

One assumption underlying all the work so far is that the disk of satellites lies in a nearly spherical potential. This is a natural choice, as orbits in spherical potentials lie in a plane. However, the disk of satellites could lie in the equatorial plane of an axisymmetric potential, or in one of the two stable principal planes of a triaxial potential (Bowden et al. 2013). We have verified by numerical calculations that the dispersal time and the number of orbits for $\Delta\phi$ to reach 2π is close to the spherical case in these instances.

Whilst our numerical simulations are simple in nature, they display qualitatively similar results to more complex simulations such as those in Libeskind et al. (2011), where Local Group substructure is shown to persist over long timescales.

4. APPLICATIONS TO GALACTIC SUBSTRUCTURE

In order to apply our results to the expected survival timescales of observed substructure, we desire a simple analytic formula for estimating a lower limit (Keplerian case) for the time taken for a clump of satellites to disperse. From eq (9), we see that

$$n_{\rm orb}\propto\frac{J}{|\delta J|}, \quad (18)$$

where ΔJ is the spread in the sum of the actions. Using our expression for the Hamiltonian, we can show

$$\delta J=\frac{GM\delta\epsilon}{2\sqrt{2}\epsilon^{\frac{3}{2}}}, \quad (19)$$

where ϵ is reduced energy. Using

$$\delta\epsilon = -\frac{GM\delta r}{r^2} - v\delta v, \tag{20}$$

we fit the functional form for the dispersal time

$$T \propto n_{\rm orb}P_{\rm orb} = A\frac{(GM)^{\frac{2}{3}}P_{orb}^{\frac{1}{3}}}{\sqrt{(\frac{GM\sigma_r}{\mu_r^2})^2 + (\mu_v\sigma_v)^2}}. \tag{21}$$

To determine the parameter A, we simultaneously fit five different orbits each with a 10x10 grid of σ_r between $2-20$ kpc and σ_v between $2-20$ kms^{-1}. The values were calculated analytically using the method described in Section 3.1. The orbital parameters for μ_r /kpc, μ_v /kms^{-1} were $[200,150]$,$[100,250]$,$[100,180]$,$[150,180]$,$[150,150]$. Using Monte Carlo methods, we recover a best fit value of $A = 0.738$. The mean absolute fractional error for the fit is 0.065, and the maximum is 0.326. The high maximum errors occurred in cases two and three, when $\mu_r = 100$ kpc and $\sigma_r = 20$ kpc. This is when we expect our approximations to break down – the Taylor expansion for calculating $\delta\omega$ is no longer valid in this regime. We only expect our formula to be applicable in the case when $\Delta J/J$ is much less than unity, ruling out for example the dispersion of structure on highly radial orbits.

4.1. *The M31 satellites*

One application of this formula is for the dispersal of a clump of satellites falling into M31. We take an M31 mass of $2\times10^{12}M_\odot$. Let us assume that an association of dwarfs of total mass of $10^{10}M_\odot$ fell into the M31 halo and was the progenitor of ~ 10 dwarf galaxies in the present-day disc of satellites. Note that the total mass in the association is rather modest, as it is smaller by a factor of ~ 10 as compared to nearby associations of dwarf galaxies studied observationally by (Tully et al. 2006). We take σ_r as 20 kpc, which, for a loosely bound clump with potential energy shape factor of 0.3, fixes σ_v at 20 kms^{-1}. In order to mimic the properties of the M31 galaxies, we place the association on an orbit with apocenter at 200 kpc and pericentre at 100 kpc. This gives an apocenter velocity of 170 kms^{-1}. In these units, this orbit has a period of 3.93 kpckm^{-1}s. Our analytic formula then gives a lower limit of 10 Gyr for the clump to disperse. This is of order the age of the universe, and we would expect this timescale to be roughly 3 times larger in a logarithmic halo.

In other words, if an association of ~ 10 dwarfs galaxies was accreted by M31 sometime within the last 10 Gyr, then we expect the association to persist rather easily and the present-day distribution would retain memory of the initial conditions. The satellites would not be fully phase-mixed and would be spread out to lie in an asymmetric disk, much as observed.

4.2. *Substructure in And II and UMi*

Another application is to the cold substructure in dwarf spheroidal galaxies, such as Andromeda II and Ursa Minor. These are probably the the result of the engulfment of smaller dwarfs and clusters within the larger dwarf spheroidal itself.

The cold stellar stream in Amorisco et al. (2014) is at a distance of roughly 1.3 kpc with a dispersion of order 0.1 kpc. The velocity dispersion is given as less than 3 kms^{-1}. The enclosed mass interior to the stream is $2.5\text{x}10^8M_\odot$. This gives a circular velocity at 1.3 kpc of 28.8 kms^{-1}. This orbit has a period of 0.3 kpc km^{-1}s. A lower limit to the dispersal timescale for these values is 450 Myr. Even for a logarithmic halo, this would suggest that, if there is a detectable angular asymmetry in the substructure, then it is relatively young. The data at this time certainly indicate that the angular extent of the stream is not a full 2π around Andromeda II, although this may be partly a consequence of the spectroscopic selection function.

The cold clump in Ursa Minor was discovered by Kleyna et al. (2003), who suggested that it may be a cluster that had fallen into the dwarf galaxy and was in the process of dissolving. As the velocity offset between the cold clump and Ursa Minor is small, this suggests that the orbit is either radial or is circular and viewed almost face-on. Kleyna et al. (2003) investigated the former possibility and showed that the dissolution timescale depended on the properties of the central parts of the potential. Here, we follow the latter possibility, namely that that cold substructure is on a near circular orbit at 150 pc from the center. The mass enclosed within the orbit is $1.25\times10^7M_\odot$. The size and the velocity dispersion of the clump are given by Kleyna et al. (2003) as 0.012 pc and 0.5 kms^{-1} respectively, which gives a phase-mixing timescale of ~ 130 Myr. This is comparable to the disruption timescale in a cusped potential found by Kleyna et al. (2003) if the clump is on a radial orbit. Note however we have probably pushed our dispersal formula to beyond its formal domain of applicability in studying disruption of such a tightly bound clump.

5. CONCLUSIONS

Our main conclusion is a general formula for the timescale for phase-mixing of orbits in nearly spherical potentials. Survival times are always shortest in Keplerian potentials and can be ~ 3 times longer in logarithmic potentials. We use the formula to demonstrate that the asymmetric distribution of the disk of satellites of M31 can be maintained without undue difficulty in nearly spherical potentials. This is because the outer parts of such galaxies have enormously long memories. If a loose association of dwarf galaxies were accreted together, then the substructure can survive for timescales longer than the age of the Universe. The accreted dwarfs would still show appreciable spatial asymmetries, much as the M31 satellites do.

AB thanks STFC for financial support. We thank the referee for a careful and thoughtful reading of the manuscript.

REFERENCES

Amorisco, N. C., Evans, N. W., & van de Ven, G. 2014, Nature, 507, 335

Bahl, H., & Baumgardt, H. 2014, MNRAS, 438, 2916

Bowden, A., Evans, N. W., & Belokurov, V. 2013, MNRAS, 435, 928
Conn, A.R., et al., 2013, ApJ, 766 120
Diaz, J., Koposov, S., Irwin, M.J., Belokurov, V., Evans, N.W., 2014, MNRAS, 443, 1688
D'Onghia, E., & Lake, G. 2008, ApJ, 686, L61
Evans, N. W., 1994, MNRAS, 267, 333
Evans, N. W., & Wilkinson, M. I. 2000, MNRAS, 316, 929
Goerdt, T., & Burkert, A. 2014, MNRAS, in press, arXiv:1307.2102
Goldstein, H., 1980, Classical Mechanics, Addison-Wesley
Kleyna, J. T., Wilkinson, M. I., Gilmore, G., & Evans, N. W. 2003, ApJ, 588, L21
Ibata, R.A., Lewis, G.F., Conn, A.R., et al. 2013, Nature, 493, 62
Li, Y.-S., & Helmi, A. 2008, MNRAS, 385, 1365
Libeskind, N. I., Knebe, A., Hoffman, Y., et al. 2011, MNRAS, 411, 1525
McConnachie, A. W., Irwin, M. J. 2006, MNRAS, 365, 902
Sadoun, R., Mohayaee, R., & Colin J. 2014, MNRAS, 442, 160
Sanders, J. L., & Binney, J. 2013, MNRAS, 433, 1813
Shaya, E. J., & Tully, R. B. 2013, MNRAS, 436, 2096
Tully, R. B., Rizzi, L., Dolphin, A. E., et al. 2006, AJ, 132, 729
Williams, A., Evans, N.W., Bowden, A. 2014, MNRAS, 442, 1405